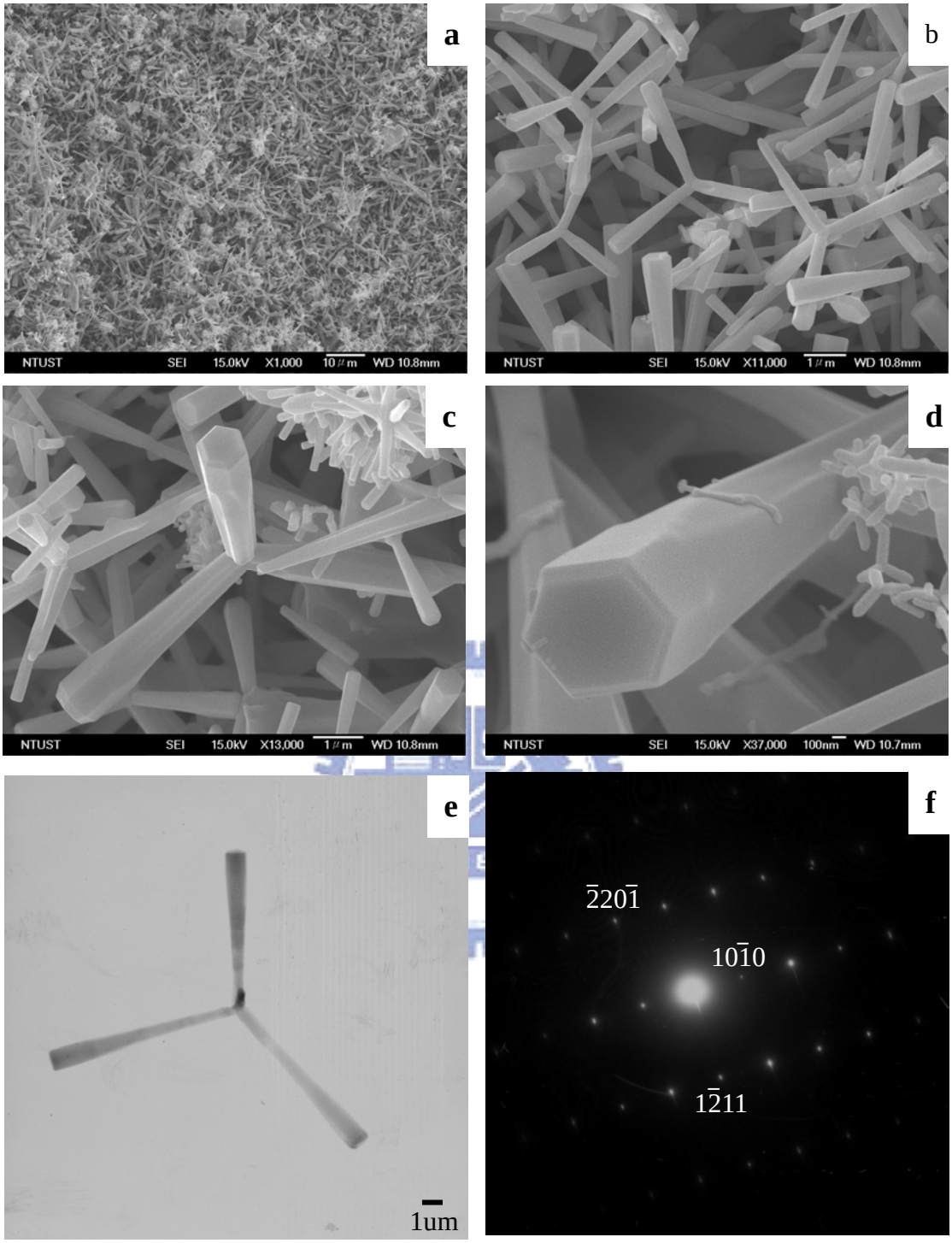

Figure 4.7 Micrographs of ZnO tetrapods grown on silicon substrate by vapor-phase-deposition at 950°C for 10min in H_2O_2 atmosphere. **a**) Low magnification, top view image of the tetrapods aggregation. **b**) A face-on view image of the bat-shape ZnO tetrapods. **c**) A bat-shape ZnO tetrapods. **d**) High magnification, title view image of the single rod of bat-shape T-ZnO. **e**) A bright-field TEM image of the bat-shape T-ZnO nanorod. **f**) A $[\bar{1}2\bar{1}6]$ zone-axis diffraction pattern of Fig. 4.7**e**.

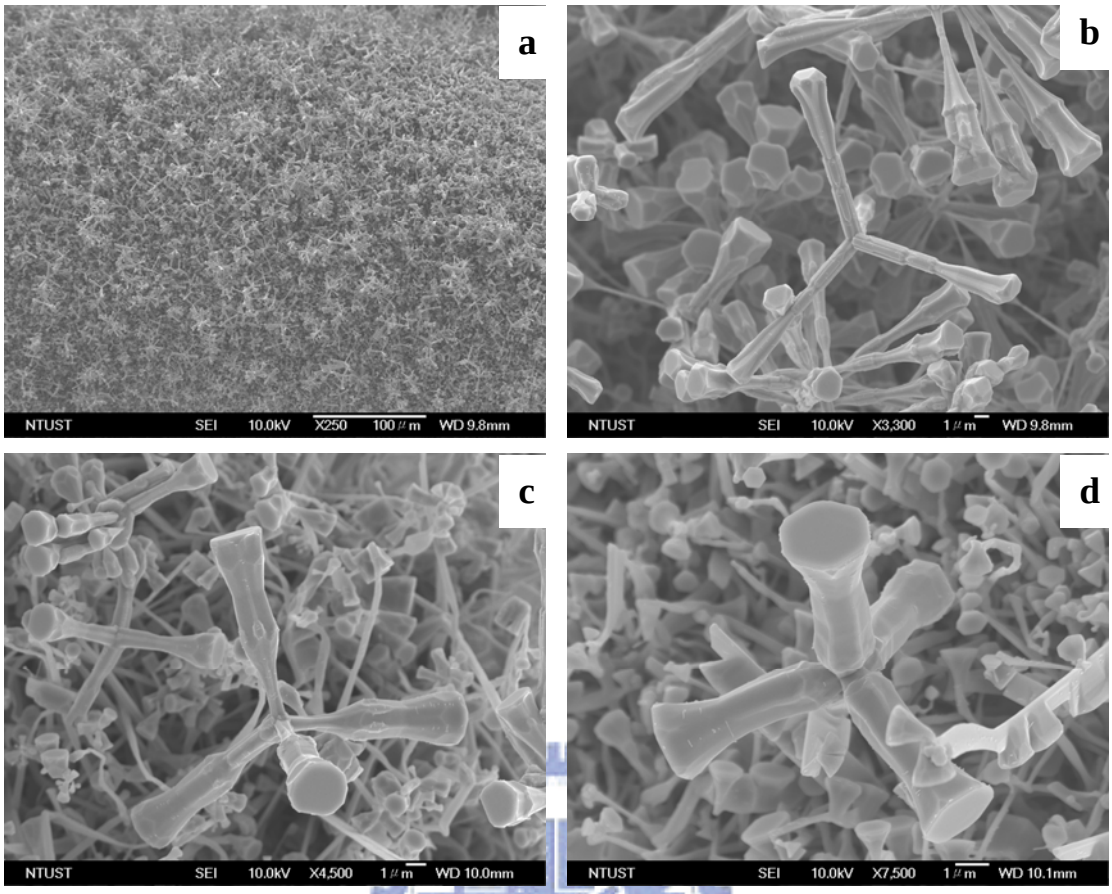

Figure 4.8 Micrographs of ZnO tetrapods grown on silicon substrate by vapor-phase-deposition at 950°C for 10min in H_2O_2 atmosphere. **a**) Top view image of large yield tetrapods on the substrate. **b**) Bamboo-shape ZnO tetrapods. **c**) Bottle-shape ZnO tetrapods. **d**) Face-on view image of the ZnO tetrapods with trumpet-shape arms.

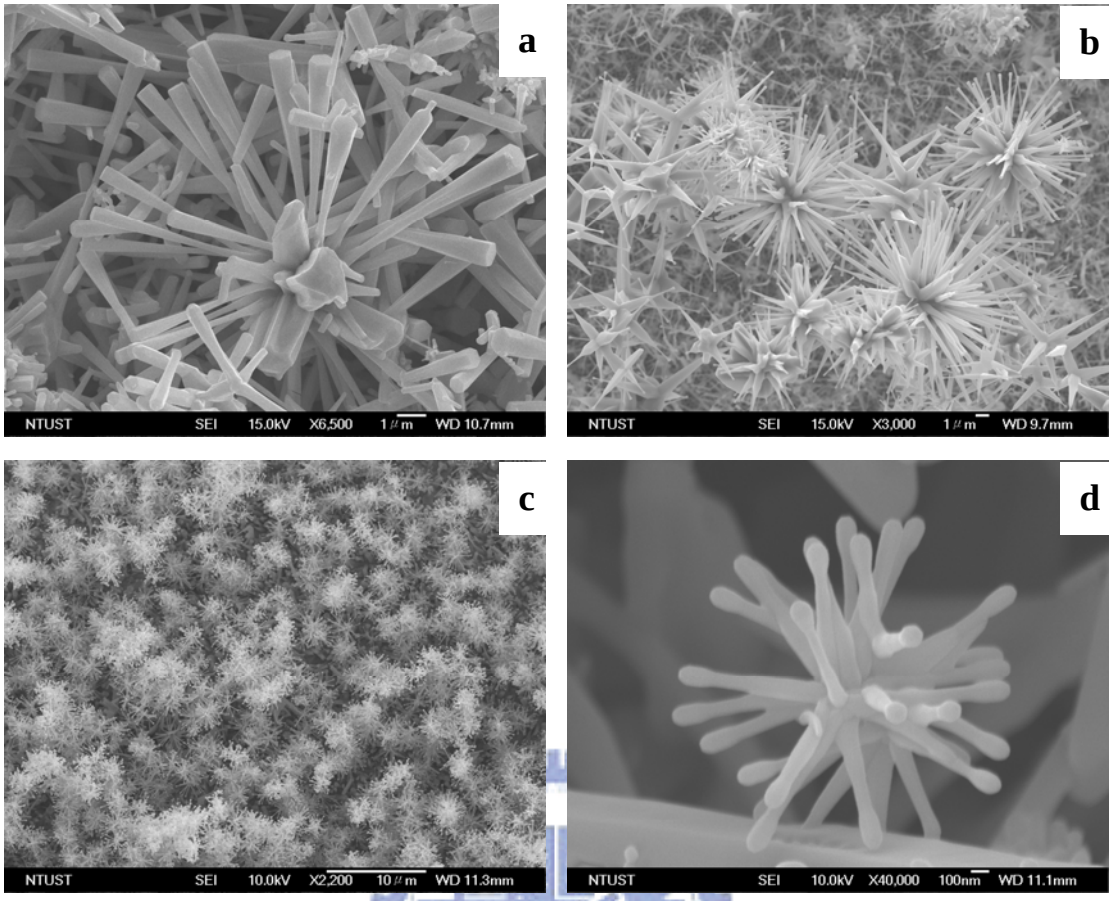

Figure 4.9 SEM micrographs of multi-rods ZnO crystals. **a**) Bat-shape ZnO multi-rods. **b**) Needle-shape ZnO multi-rods. **c**) Low magnification, face-on view image of multi-rods ZnO crystals **d**) Freestanding anemone-shape ZnO crystal.

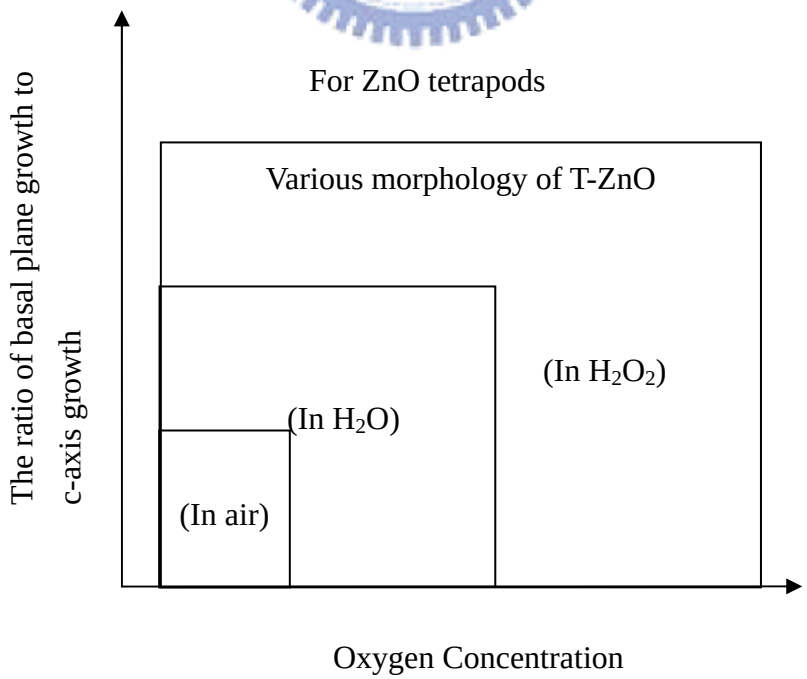

Figure 4.10 A schematic chart of the oxygen concentration v.s. the ratio of basal plane growth to c-axis growth.

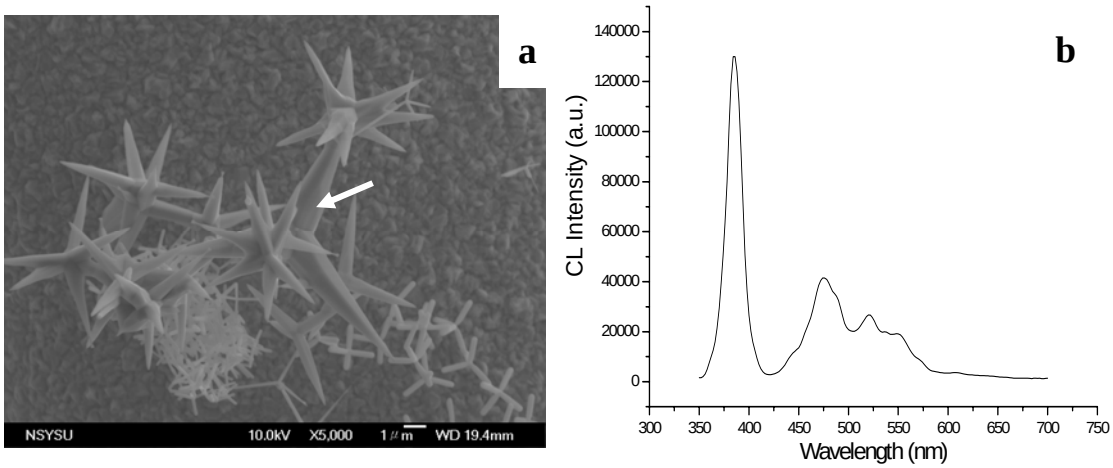

Figure 4.11 SEM micrographs correspond to CL spectra for ZnO tetrapods synthesized in air atmosphere. The ZnO tetrapods dispersed on the Cu net for TEM recorded. **a**) The arrow in Fig. 4.11**a** points to CL detection for the individual ZnO tetrapods crystal. **b**) CL spectrum of the individual ZnO tetrapods in Fig.4.11**a**.

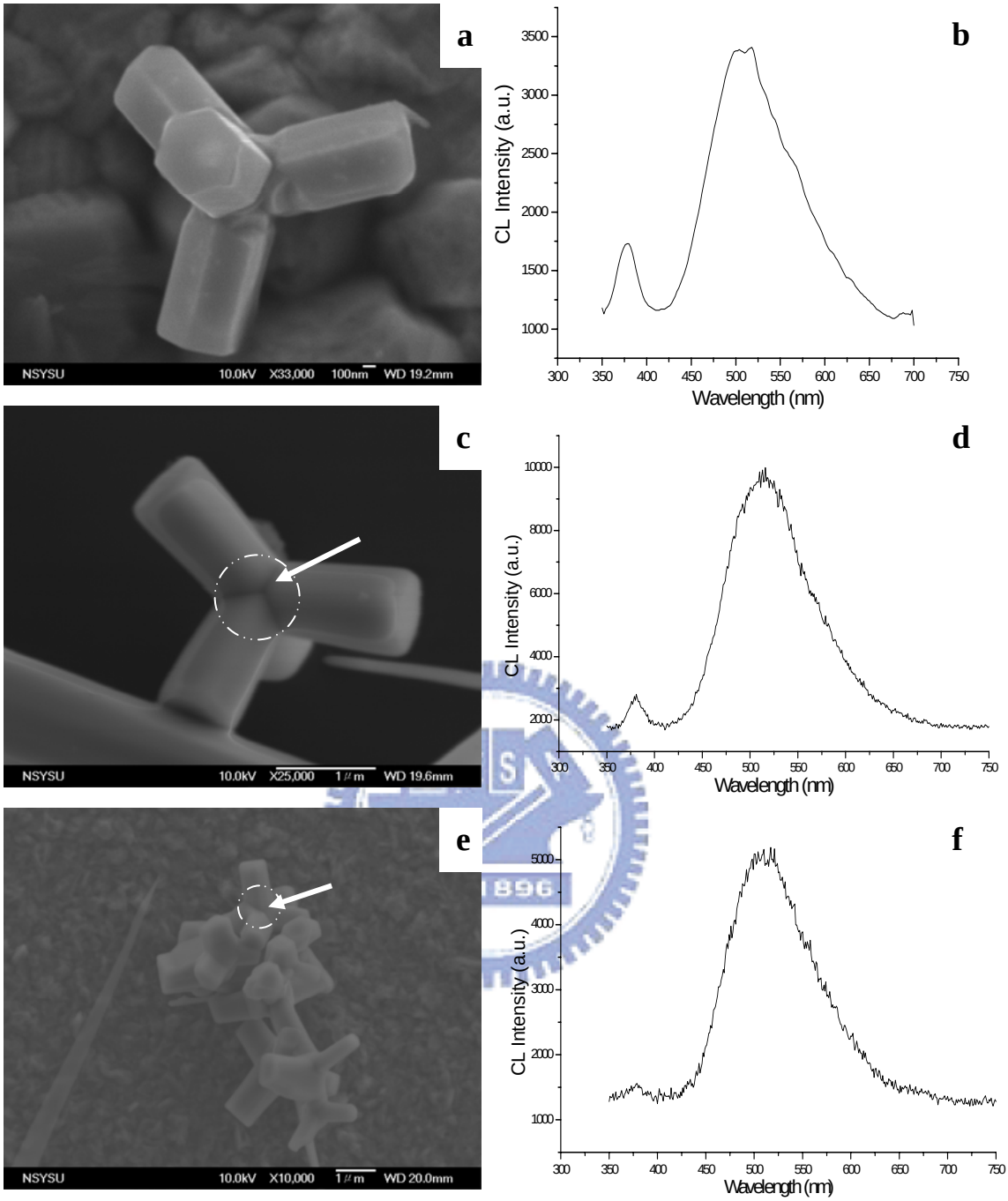

Figure 4.12 SEM micrographs of the ZnO tetrapods with similar diameter in shape by synthesized in H_2O atmosphere correspond to CL spectra. **a**) Face-on view image of the freestanding ZnO tetrapods. **b**) CL spectrum of the single ZnO tetrapods in Fig. 4.12**a**. **c**) Face-on view image of the single ZnO tetrapods. **d**) The arrow in Fig. 4.12**c** points to CL detection for the individual ZnO tetrapods. **e**) Face-on view image of the aggregately ZnO tetrapods. **f**) The arrow in Fig. 4.12**e** points to CL detection for the individual ZnO tetrapods.

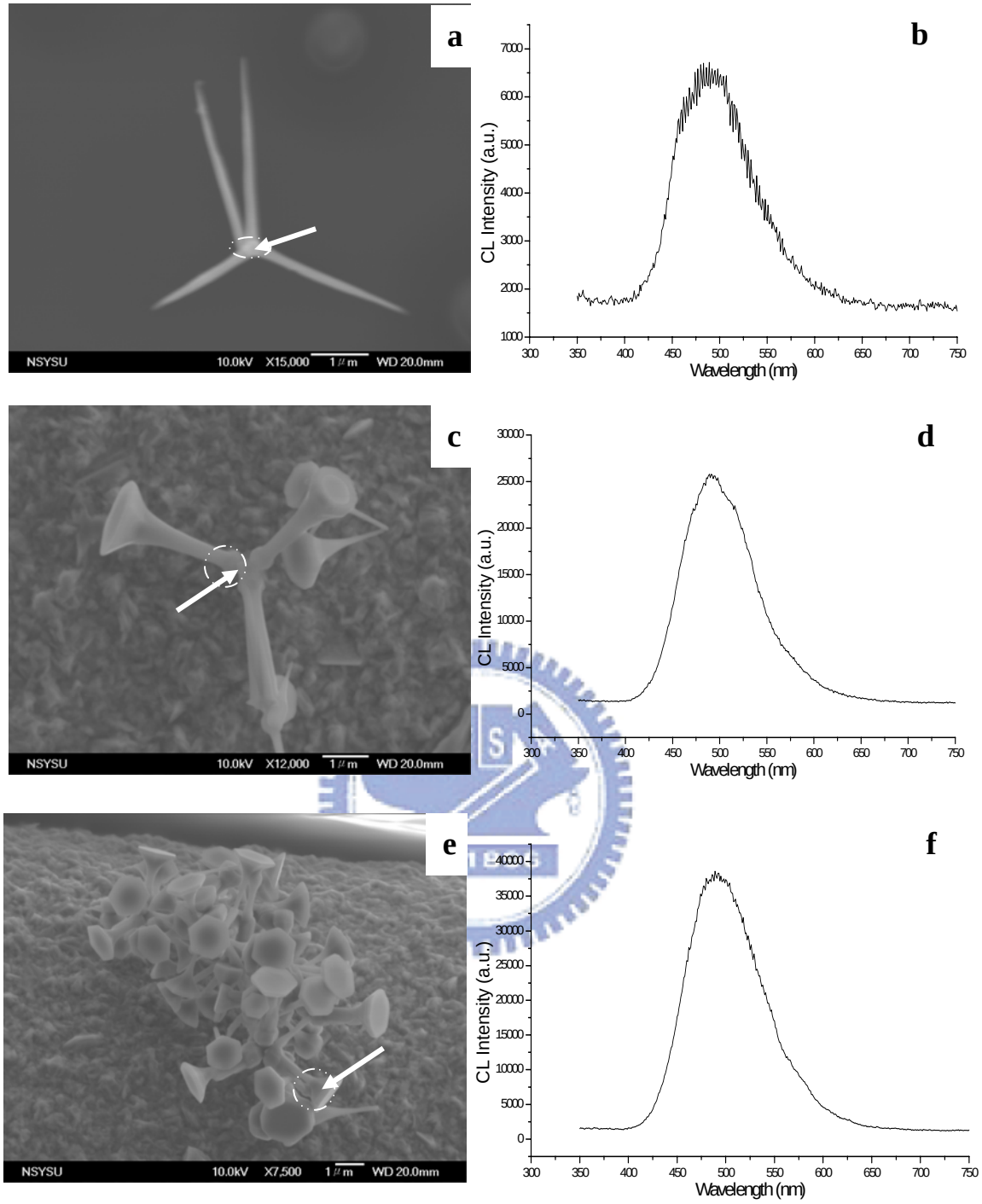

Figure 4.13 SEM micrographs and corresponding to CL spectra of ZnO tetrapods synthesized in H_2O_2 atmosphere. **a**) Face-on view image of the freestanding ZnO tetrapods. **b**) The arrow in Fig. 4.13**a** indicates the point to CL detection of the freestanding ZnO tetrapods. **c**) Top view image of the single ZnO tetrapods. **d**) The arrow in Fig. 4.13**c** indicates the point to CL detection for the individual ZnO tetrapods. **e**) Face-on view image of the aggregately ZnO tetrapods. **f**) The arrow in Fig. 4.13**e** points to CL detection for the individual ZnO tetrapods.

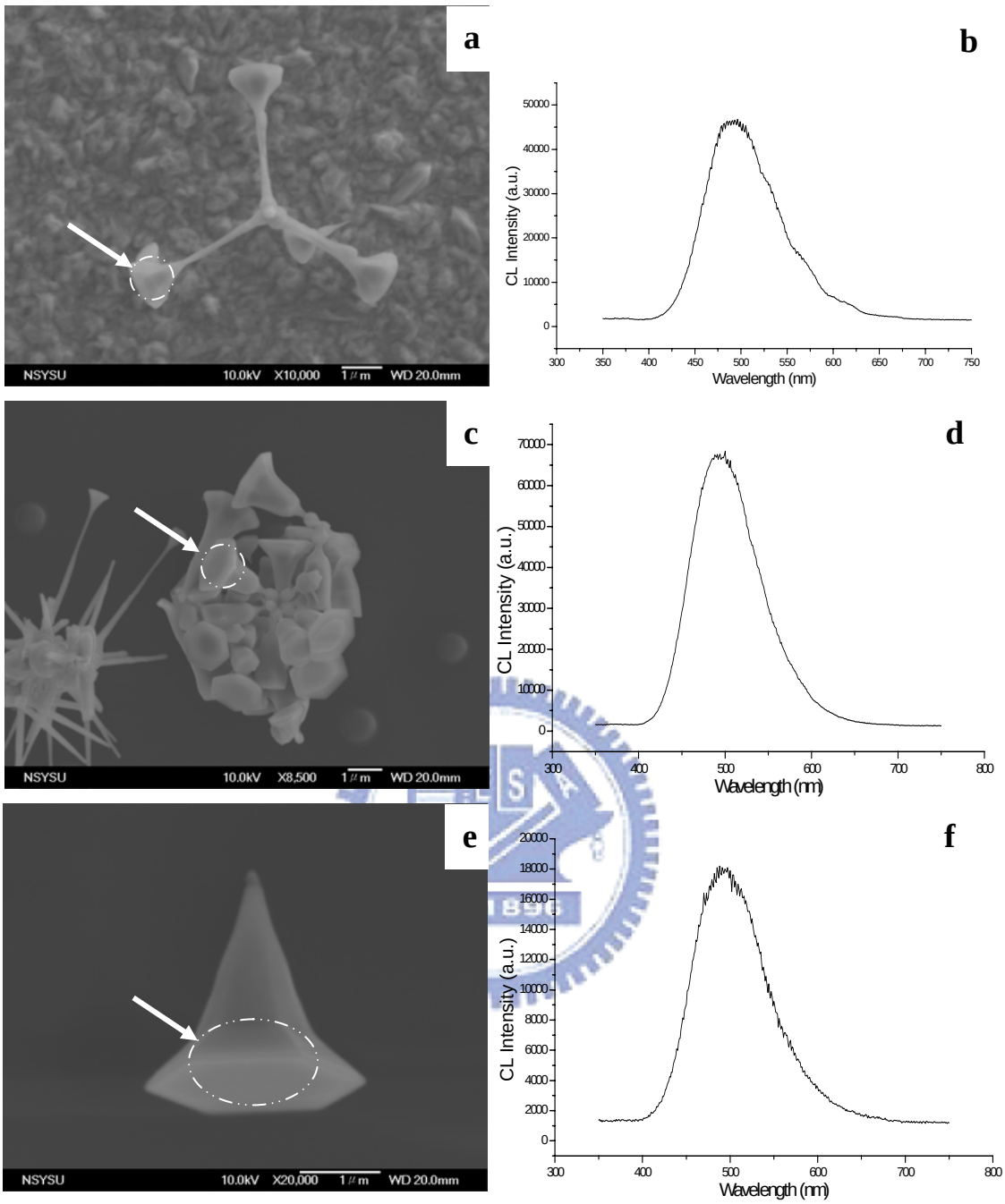

Figure 4.14 SEM micrographs and corresponding to CL spectra of ZnO tetrapods synthesized in H_2O_2 atmosphere. **a**) Face-on view image of the freestanding ZnO tetrapods. **b**) The arrow in Fig. 4.14**a** points to CL detection for the individual ZnO tetrapods. **c**) Aggregated bell-shape ZnO crystals. **d**) The arrow in Fig. 4.14**c** points to CL detection for the individual ZnO crystal. **e**) Freestanding diamond-shape ZnO crystal. **f**) The arrow in Fig. 4.14**e** points to CL detection of the individual ZnO crystal.

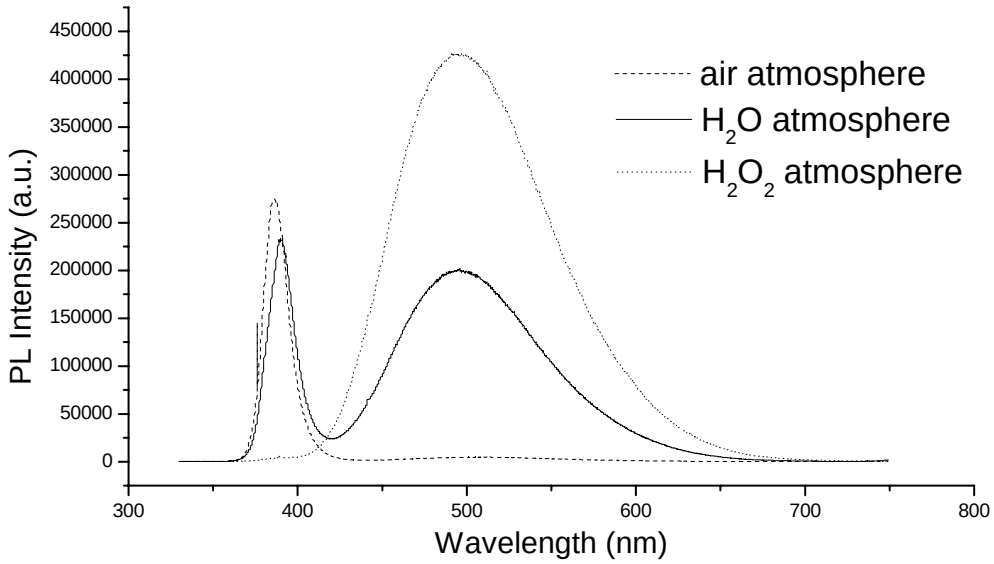

Figure 4.15 ZnO tetrapods synthesized in three ambiences exhibited different PL spectra.